# Supplementary Materials for

## Tissue-resident memory T cell maintenance during antigen persistence requires both cognate antigen and interleukin-15

Roger Tieu, Qiang Zeng, Daqiang Zhao, Gang Zhang, Neda Feizi, Priyanka Manandhar, Amanda L. Williams, Benjamin Popp, Michelle A. Wood-Trageser, Anthony J. Demetris, J. Yun Tso, Aaron J. Johnson, Lawrence P. Kane, Khodor I. Abou-Daya, Warren D. Shlomchik, Martin H. Oberbarnscheidt, Fadi G. Lakkis

correspondence to: mho6@pitt.edu; lakkisf@upmc.edu

**This PDF file includes:**

Supplementary Methods
Figs. S1 to S7

**Other Supplementary Materials for this manuscript includes the following:**

Reagent list Table_S1.xlsx

## Supplementary Methods

*Analysis of intragraft myeloid cells*

t-Distributed Stochastic Neighbor Embedding (t-SNE) dimension reduction, FlowSOM (*86*), and ClusterExplorer analyses were performed in FlowJo. t-SNE analyses were performed on concatenated data from kidney allograft and spleen using all markers not utilized for manual gating (e.g. viability). As noted in Fig. S5C, clusters of less than 5% frequency (of the total leukocytes) were not labelled with a phenotype. A conservative cut-off was chosen in order to avoid misidentification of populations or classification of non-bona fide populations.

*Statistical Analysis*

Nonlinear regression analysis using Prism (GraphPad) was used to model resident memory T cell population kinetics data, using data points between 4 and 56 days post-transplantation. Model constraints imposed that decay plateau = 0 and a positive rate constant. Either one-phase or two-phase exponential decay models were selected after comparison using the Akaike information criterion.

## Supplementary Figures

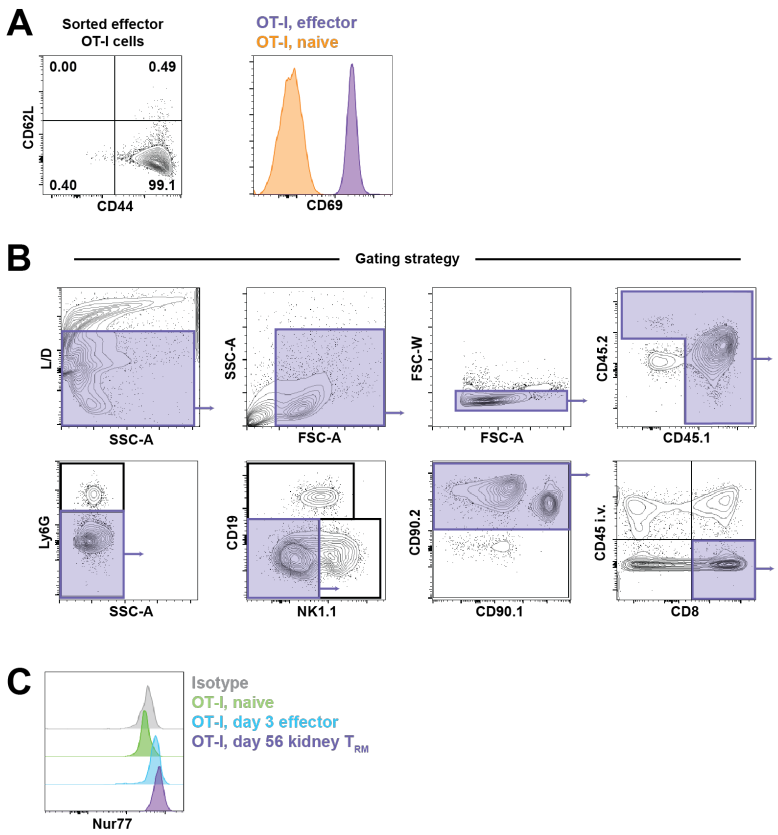


**Figure S1. Gating strategy for $T_{RM}$ cells in renal allograft tissue.**
(A) Phenotype of effector OT-I cells used for adoptive transfers.
(B) Granulocytes, NK cells, and B cells were excluded by gating out Ly-6G, NK1.1, and CD19-expressing cells, respectively. T cells were analyzed by gating on CD90.2-expressing cells. Extravascular CD8 T cells were excluded by gating on $CD8^{+}CD45i.v.^{-}$ cells. Passenger donor T cells ($CD45.2^{+}CD90.2^{+}$) were extremely rare in the graft tissue at all time points (<1% of all extravascular $CD45^{+}$ cells).
(C) Representative plot of Nur77 intracellular staining from isotype control (gray), naïve OT-I cells (green), effector OT-I cells generated after 3 days activation (blue), or $T_{RM}$ OT-I cells from renal allograft tissue 56 days post-transplantation (purple).

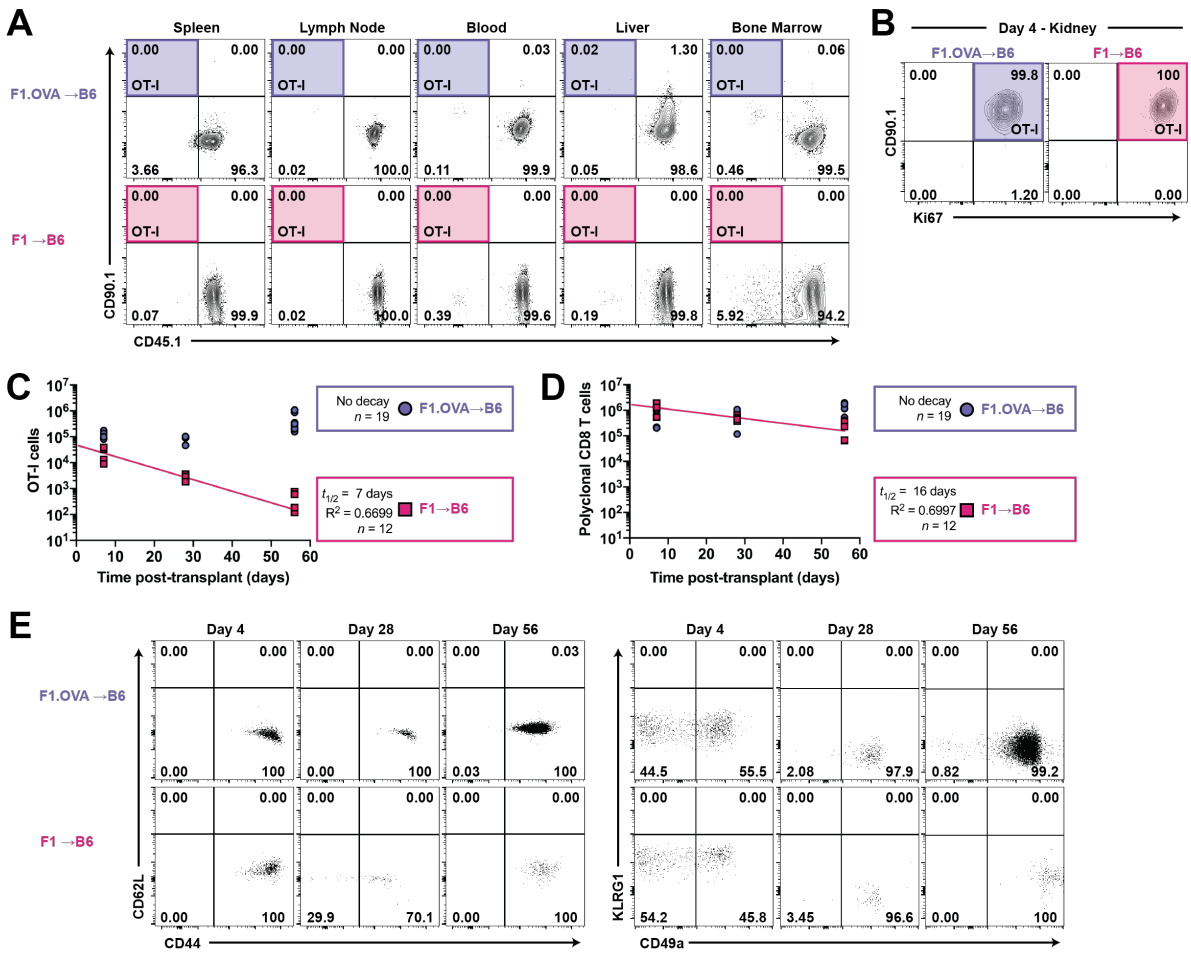


**Figure S2. Effector OT-I cells infiltrate renal allograft tissue in the absence of cognate antigen and take up residence only in the graft.**

(A) Percentage (representative plots) of OT-I cells in various tissues from recipients of either F1.OVA (top row, purple) or F1 (bottom, magenta) renal allografts at day 56 post-transplantation. *n* = 4-5 mice per group.

(B) Representative plots of Ki67-expressing intragraft OT-I cells at day 4 post-transplantation. *n* = 4 mice per group.

(C, D) Enumeration of CD90.1$^{+}$ OT-I cells (C) and polyclonal CD8 (D) in renal allograft tissue at days 4, 28, and 56 post-transplantation. Linear regression and associated model details are shown. *n* = 4-8 mice per group per time point.

(E) Cell surface phenotype of intragraft OT-I cells at days 4, 28, and 56 post-transplantation.

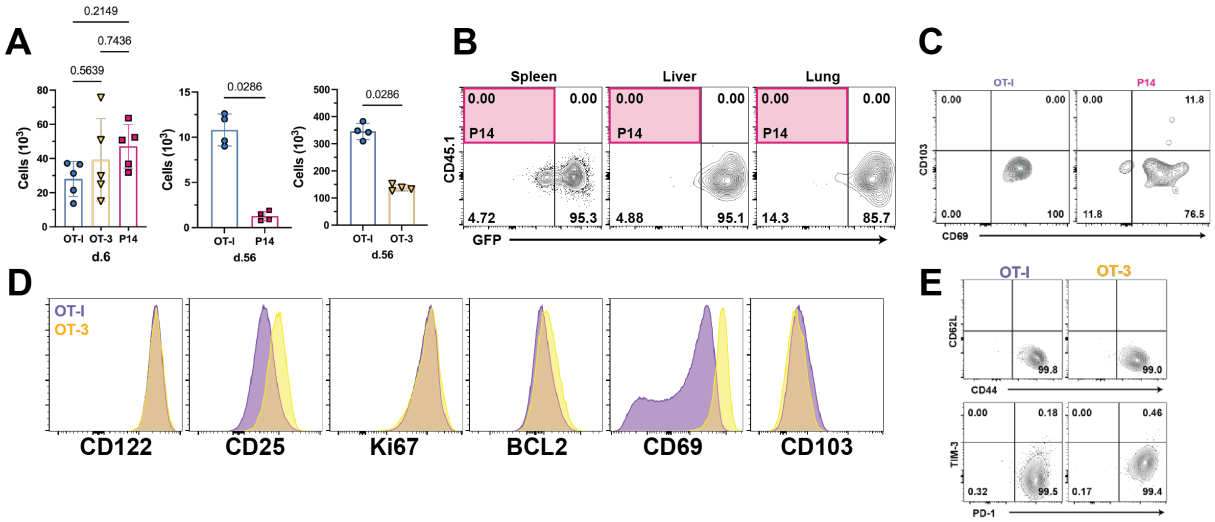


**Figure S3. Co-adoptive transfer of effector P14 or OT-3 cells with effector OT-I cells.**
(A) Absolute numbers of co-transferred OT-I, P14, and/or OT-3 cells present in the graft on days 6 and 56 after transplantation.
(B) Percentage (representative plots) of P14 cells in various tissues at day 56 post-transplantation.
(C) Phenotype of graft P14 T cells on d.56 post-transplantation.
(D) Histogram plots of various markers of signaling, function, activation, and adhesion (CD103) in effector OT-I (red) and effector OT-3 (blue) cells. *n* = 4 mice per group.
(E) Phenotype of graft OT-3 cells on d.56 post-transplantation.

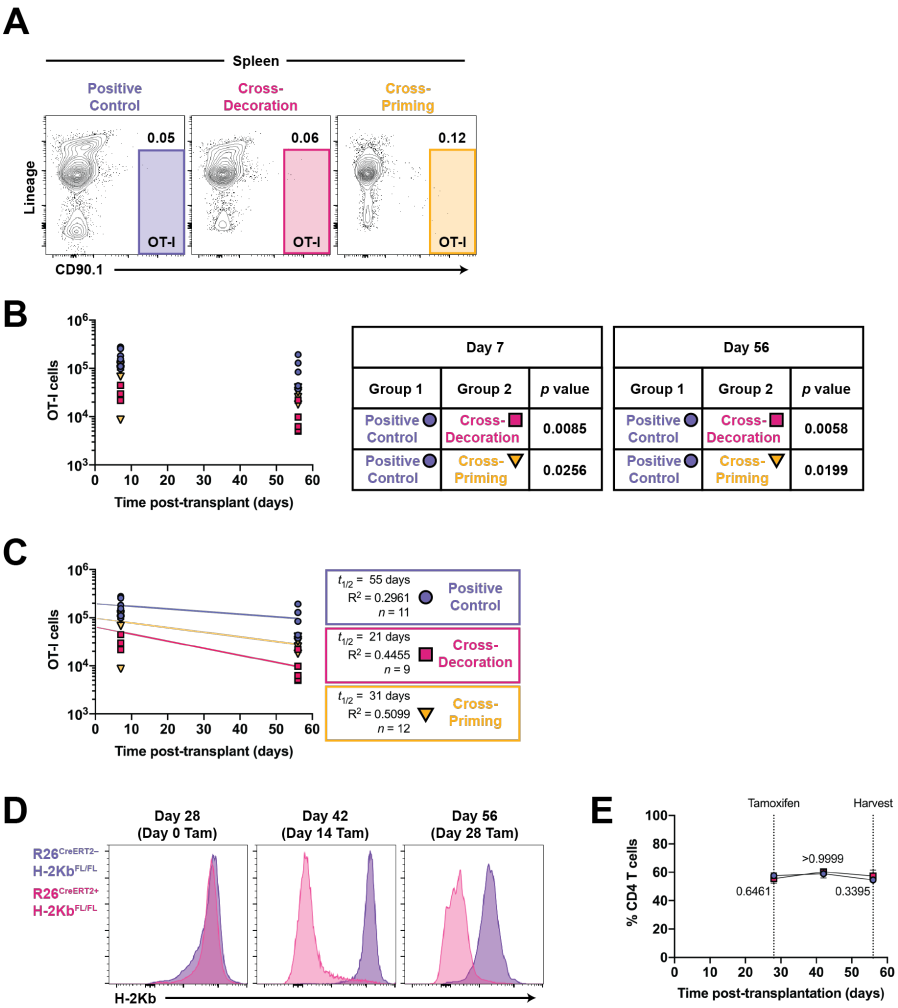


**Figure S4. $T_{RM}$ OT-I cells decay in the absence of cognate antigen presentation and do not egress from renal allograft tissue.**

(A) Percentage (representative plots) of OT-I cells in spleen at day 56 post-transplantation.

(B, C) Enumeration of CD90.1$^{+}$ OT-I cells in renal allograft tissue at days 7 and 56 post-transplantation. (B) *P* values for comparison of groups per time point are shown. (C) Linear regression and associated model details are shown. *n* = 5-6 mice per group per time point.

(D) Representative histograms of H-2Kb expression of peripheral blood lymphocytes after tamoxifen treatment.

(E) Percentage of CD4 T cells in peripheral blood after tamoxifen treatment.

*P* values were determined by (B) one-way ANOVA with Tukey's correction, and (E) two-tailed unpaired t test.

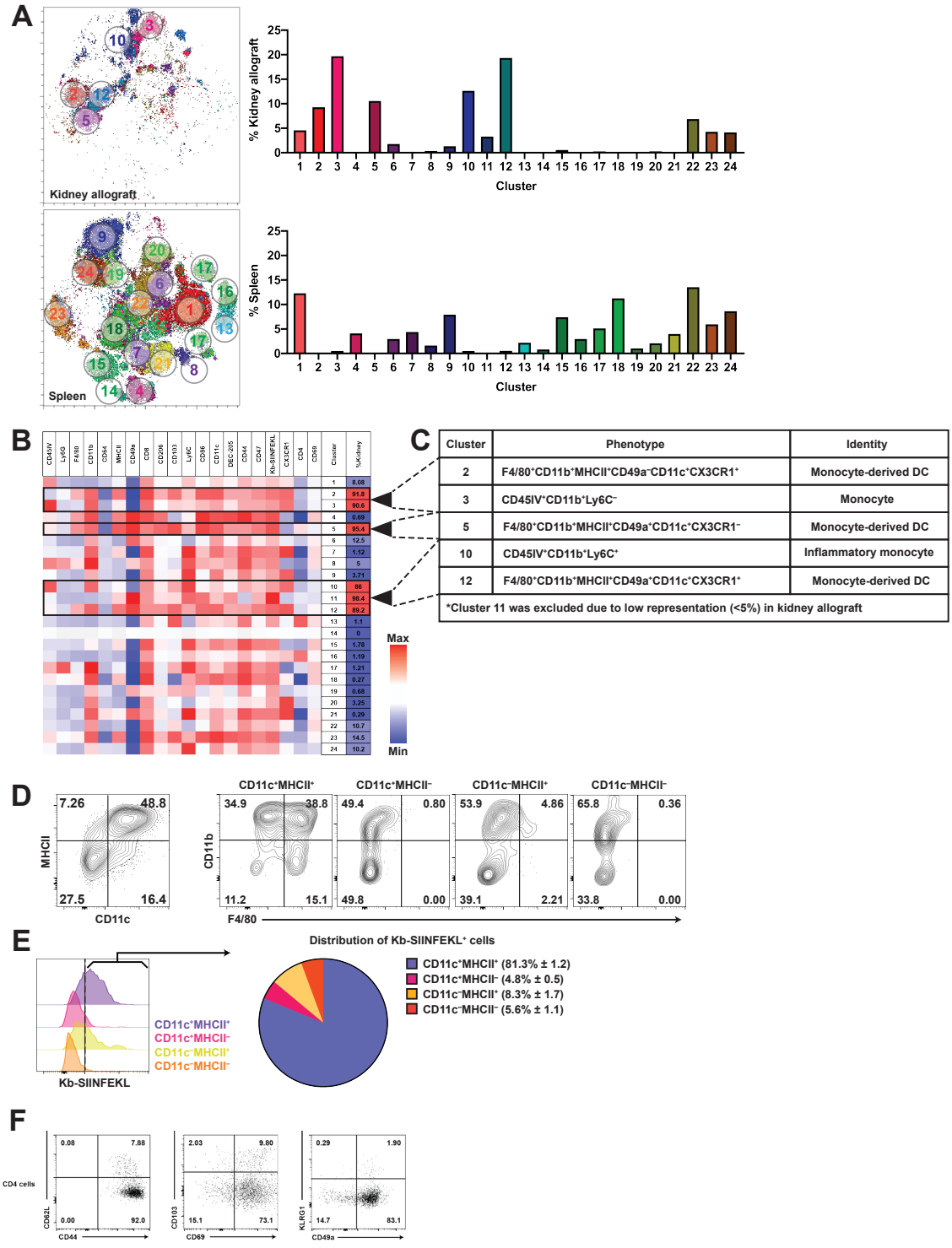


**Figure S5. Graft-infiltrating DCs are heterogeneous and are the primary APC in graft tissue.** (A) (Left) t-Distributed stochastic neighbor embedding (t-SNE) plot of myeloid cells from (left, top) kidney allograft and (left, bottom) spleen tissue at day 56 post-transplantation. NK cells, B cells, and T cells were excluded by gating out NK1.1, CD19, CD90.1, and CD90.2-expressing cells. Donor cells were excluded by gating on GFP$^+$ cells. Percent representation of each cluster to either (right, top) kidney allograft or (right, bottom) spleen. *n* = 4 mice.
(B) Heatmap of cell surface marker expression for each cluster.

(C) Table of clusters unique to myeloid cells from kidney allograft tissue. Cluster 11 was excluded due to low representation (<5%).
(D) (Left) Flow plot of myeloid cells for CD11c and MHCII. (Right) Flow plots of various gates for F4/80 and CD11b.
(E) (Left) Histogram plot of Kb-SIINFEKL on various myeloid cell populations. (Right) Pie chart of various myeloid cell populations expressing Kb-SIINFEKL as a fraction of total myeloid cells.
(F) Phenotype of polycolonal CD4 T cells in the graft on d.56.

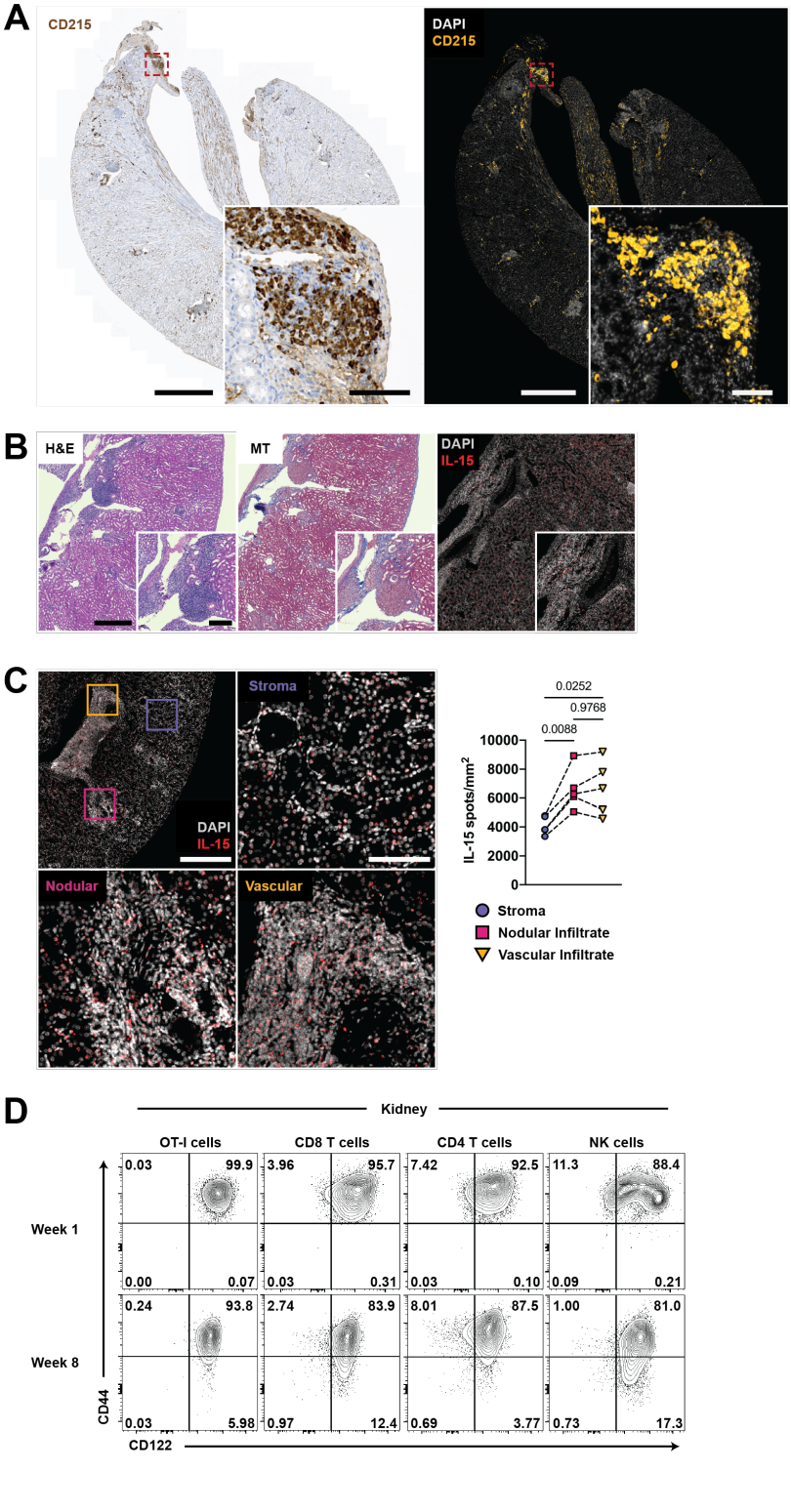


**Figure S6. IL-15 signaling takes place in renal allograft tissue.**

(A) Expression of CD215 in renal allograft tissue at day 56 post-transplantation by (left) chromogen and (right) immunofluorescent staining. Whole image scale bar: 1000 μm. Cropped inset scale bar: 100 μm.
(B) H&E, Masson's trichrome, and fluorescent *in situ* hybridization IL-15-stained sections of F1.OVA renal allograft tissue at day 56 post-transplantation. Whole image scale bar: 500 μm. Cropped inset scale bar: 200 μm. $n$ = 5 mice.
(C) Representative staining for IL-15 mRNA in stroma, nodular infiltrates, and vascular infiltrates. Quantification of IL-15 spots in various areas of interest. Whole image scale bar: 500 μm. Areas of interest scale bar: 100 μm.
(D) Representative flow plots of CD122 expression on T cells from day 7 (top) and 56 (bottom) post-transplantation. NK cells shown as a positive control. $n$ = 6-8 mice per group.
*P* values were determined by (C) mixed-effects model with Tukey’s correction.

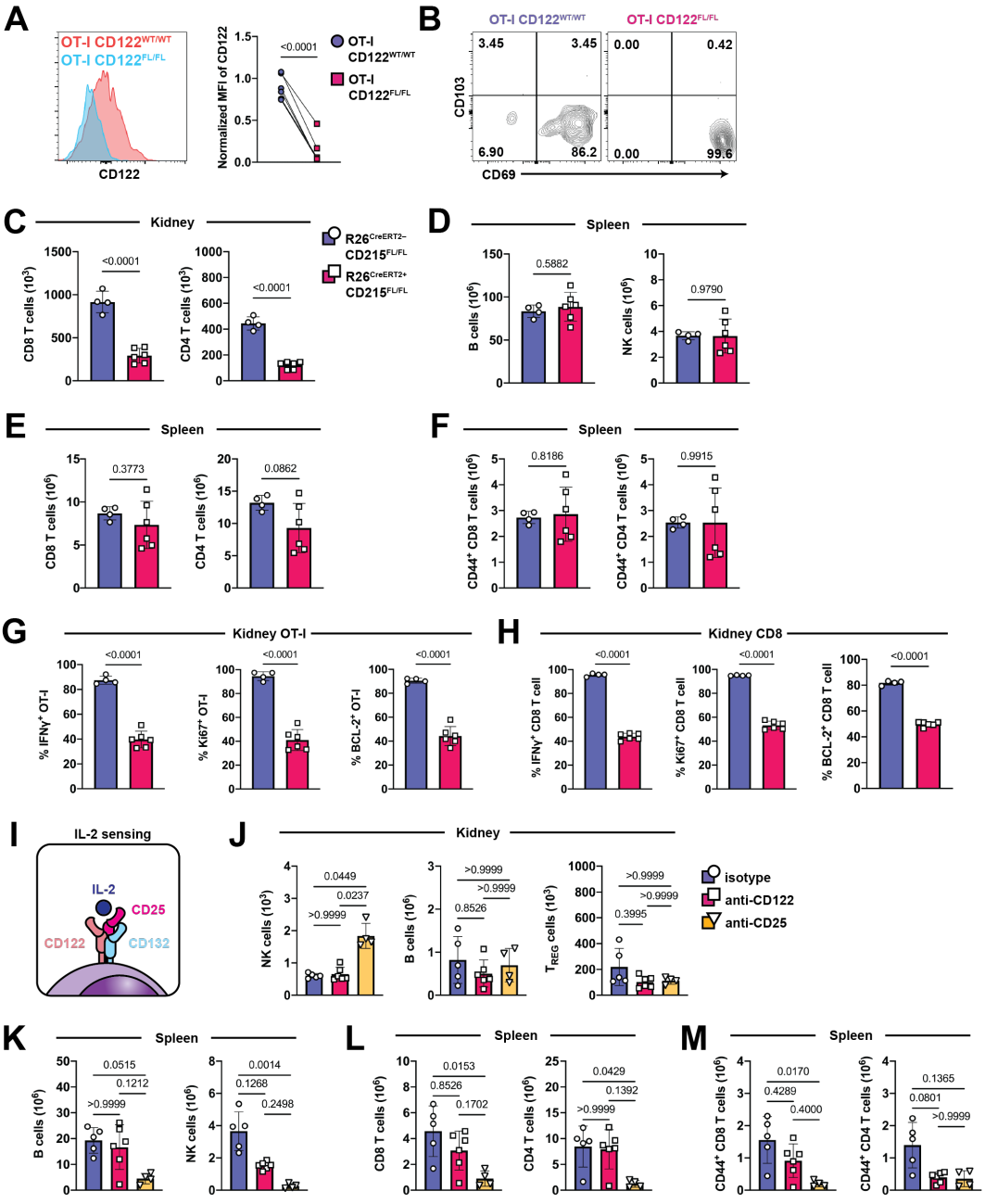


**Figure S7. Genetic ablation and antibody blockade of IL-15 signaling.**
(A) (Left) Histogram plot and (Right) normalized MFI of CD122 on OT-I WT and OT-I CD122$^{FL/FL}$ R26$^{CreERT2+}$ cells after tamoxifen treatment at day 56 post-transplantation. *n* = 6 mice.
(B) Representative flow plots for CD69 and CD103 expression of OT-I WT and OT-I CD122$^{FL/FL}$ R26$^{CreERT2+}$ cells.
(C-E) Absolute number of splenic (D) B and NK cells, (E) total CD8 and CD4 T cells, and (F) CD44$^{+}$ CD8 and CD4 T cells from CD215$^{FL/FL}$ recipients.
(F) Frequency of polyclonal CD8 $T_{RM}$ cells for expression of IFNγ, Ki67, and BCL2 after overnight restimulation with donor F1.OVA splenocytes.
(G) Schematic of IL-2 signaling.

(H) Absolute number of intragraft NK cells, B cells, and FOXP3$^{+}$ regulatory T cells after antibody treatment at day 42 post-transplantation. *n* = 4-6 mice per group
(I-K) Absolute number of splenic (I) B cells and NK cells, (J) total CD8 and CD4 T cells, and (K) CD44$^{+}$ CD8 and CD4 T cells after antibody treatment at day 42 post-transplantation.
*P* values were determined by (A) two-tailed paired t test, (C-F) two-tailed unpaired t test, and (H-K) Kruskal–Wallis one-way ANOVA with Dunn's correction.